A process and control simulator for large scale cryogenic plants

Benjamin Bradu, Silviu-Iulian Niculescu, Philippe Gayet

A process and control simulator for large scale cryogenic plants

Benjamin Bradu[a,b,*], Philippe Gayet[a,1], Silviu-Iulian Niculescu[b,2]

[a] *CERN, CH-1211 Genève 23, Switzerland*
[b] *Laboratoire des Signaux et Systèmes, UMR CNRS 8506, CNRS-Supélec, 3 rue Joliot Curie, 91192, Gif-sur-Yvette, France*

Abstract

This paper presents a process and control simulator for industrial helium cryogenic plants controlled by Programmable Logic Controllers (PLC). This simulator can be used for different purposes such as operator training, test of the PLC programs or the optimization of the plant. The different component models used in the simulator are detailed and explained. Various large scale cryogenic plants used for the particle accelerator LHC (Large Hadron Collider) at CERN have been modeled and simulated. The good agreement between the simulation results and the dynamic behaviour of real plants is demonstrated with experimental results. Various discussions complete the presentation.

Key words: Cryogenics, Dynamic models, Simulation, Thermodynamics, operator training

1. Introduction

In 2008, the European Organization for Nuclear Research (CERN) started the most powerful particle accelerator of the world, the Large Hadron Collider (LHC). The LHC accelerates proton beams which are driven by superconducting magnets maintained at 1.9 K over a 27 km ring. To cool-down and maintain superconductivity, large helium refrigeration plants are used, see Lebrun (1999) for more details.

Large scale cryogenic plants are continuous industrial processes, very similar to petroleum (Olsen, Endrestol, and Sira, 1997), chemical (Szafnicki, Narce, and Bourgois, 2004) or sugar industries (Alves, Normey-Rico, Merino, Acebes, and de Prada, 2005). They are composed with the same kind of components (heat exchangers, valves, turbines, compressors, phase separators, etc.) but with additional constraints due to very low temperatures.

Cryogenic plants and their control are highly complex due to the large number of correlated variables on wide operation ranges. Currently, the design and the control of cryogenic systems are based on CERN and suppliers' experience on the process and on appropriate "static" calculations. Due to the complexity of the systems (coupled partial differential equations, propagation and transport phenomena), dynamic simulations represent the only way to provide adequate data during transients.

A new dynamic simulator, PROCOS (PROcess and COntrol Simulator), has been developed to improve knowledge on complex cryogenic systems (Bradu, Niculescu, and Gayet, 2008b). The main objectives of the proposed simulator can be summarized as follows: the operator training, the test of control programs on "virtual" plants before their implementation (virtual commissioning) and the test of new control strategies to optimize the overall behavior of complex systems. This simulator is able to simulate large refrigeration plants using helium and connected to the actual control system of CERN. Furthermore, the existing control policy and supervision systems can be fully reused in simulation. Some advanced control developments as predictive control have already been studied for some LHC cryogenic systems (Blanco, de Prada, Cristea, and Casas, 2009) but it has not been implemented yet and this dynamic simulator can be used to demonstrate efficiency of such controllers.

The superconducting magnets of the LHC were successfully cooled at 1.9 K during 2008. The real operation of the cryogenic plants has started and the use of a dynamic simulator is now the only way to test new control strategies in order to enhance the cryogenic systems

*corresponding author. Tel : +41 22 76 74446; fax.:+41 22 76 68274

Email addresses: benjamin.bradu@cern.ch (Benjamin Bradu), philippe.gayet@cern.ch (Philippe Gayet), niculescu@lss.supelec.fr (Silviu-Iulian Niculescu)

[1] Fax : +41 22 76 68274

[2] Fax : +33 1 69 85 17 65

without disturbing the LHC operation.

First, various studies devoted to the simulation, analysis and design of cryogenic plants are presented. Next, the simulation approach is outlined in Section 2 and various comparisons with the existent results are proposed. A particular attention has been paid to the simulation architecture and on the explicit modelling approach of the components. Next, simulation results are detailed (CMS cryoplant at 4.5 K and 1.8 K unit for the LHC), compared with experimental data and discussed (simulation speed and some comparisons) in Section 4. Some concluding remarks and perspectives end the paper.

2. Process and Control simulation approach

2.1. Existing cryogenic modelling approaches

In various fields of industry, dynamic simulators have been developed to train operators or to design new control techniques, see Alves et al. (2005); Olsen et al. (1997); Szafnicki et al. (2004). To the best of the authors' knowledge, there exists only a few dynamic simulations devoted to helium cryogenic plants:

- Maekawa, Ooba, Nobutoki, and Mito (2005) have simulated a 10 kW @ 4.5 K refrigerator used in a fusion experiment;
- next, Butkevich, Idnic, and Shpakov (2006) developed an educational training tool on an helium liquefier;
- Kutzschbach, Haberstroh, and Quack (2006) have simulated a commercial helium liquefier;
- finally, Deschildre, Barraud, Bonnay, Briend, Girard, Poncet, Roussel, and Sequeira (2008) made simulations on a 800 W @ 4.5 K refrigerator.

The proposed simulation approach presents some similarities with the above simulators but it shows also new features and concepts. All simulators perform dynamic simulations by using an object oriented modelling where each cryogenic component is individually modeled by physical differential and algebraic equations (DAEs), excepting the simulator of Butkevich et al. (2006) which is based on mathematical and heuristic modelling.

To model CERN cryogenic systems, a commercial modelling and simulation software was used: EcosimPro© (EA Internacional, 2007). This software was chosen for its flexibility and its ability to export models in C++ classes in order to embed models in larger simulation environments.

All cryoplants that have been modeled are large-scale cryogenic systems. In the adopted object approach, the number of equations is proportional to the number of objects: the complexity of the model is directly linked to the number of the main components, namely the heat exchangers (HXs) and turbines. In terms of numerical computation, large-scale systems can be defined for cryogenic plants containing more than 5 HXs and more than 2 turbines. This configuration generates around 1500 DAEs and it corresponds to a helium refrigerator with a refrigeration power of 400 W at 4.5 K.

All existing simulators have been used only to model helium liquefiers or 4.5 K helium refrigerators. Here, in addition to 4.5 K refrigerators, the modelling was extended to a 1.8 K refrigeration unit using cold-compressors.

Simulations are generally including a simplified control in the model. Therefore, most of existing simulators are not taking into account the real process control and cannot be used as a real-time training simulator, except the simulator of Maekawa et al. (2005). The originality of PROCOS resides in the fact that it is based on the real process control architecture including the supervision system. The process and the control duties are simulated separately and synchronized together. Hence, it allows the simulation of large-scale systems on several computers by decoupling main parts of a plant.

2.2. Simulation architecture

All CERN cryogenic systems are controlled by industrial Programmable Logic Controllers (PLCs). The control architecture and the control policy are based on an object-oriented hierarchical multilevel and multilayer control framework developed at CERN and called UNICOS. This control framework is based on the IEC 61512 control standard (IEC, 1997), for a complete description of the control system, see Gayet and Barillère (2005).

PROCOS reproduces the UNICOS architecture in simulation even for the three hardware layers as it is shown in the Fig. 1. The supervision layer remains the same with operator consoles, PLCs which perform the control are replaced by PLC simulators (softwares) provided by PLC manufacturers and the cryogenic plant is replaced by a cryogenic process simulator integrating *physical equations* of the system.

The same PLC I/O names are used in the process model (inputs are sensors and outputs are actuators). Hence, an OPC server can be configured automatically to establish the link between the PLC and the model. A lot of time can be saved for large applications, see Fig. 2.

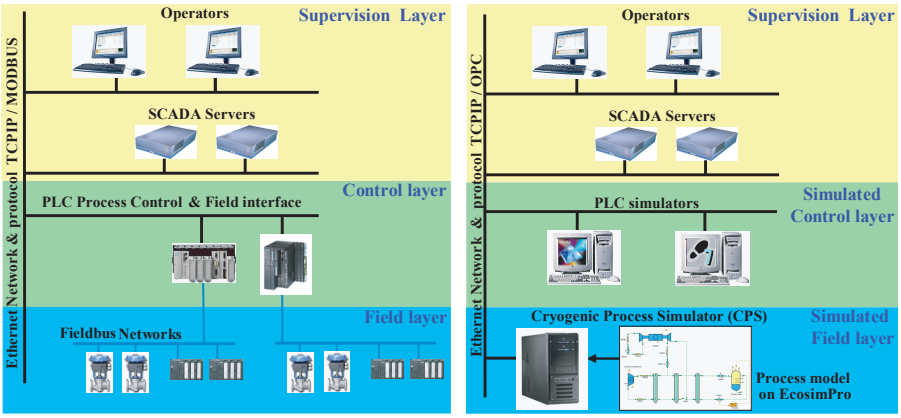

Figure 1: The real and the simulated control architecture for CERN cryogenic systems

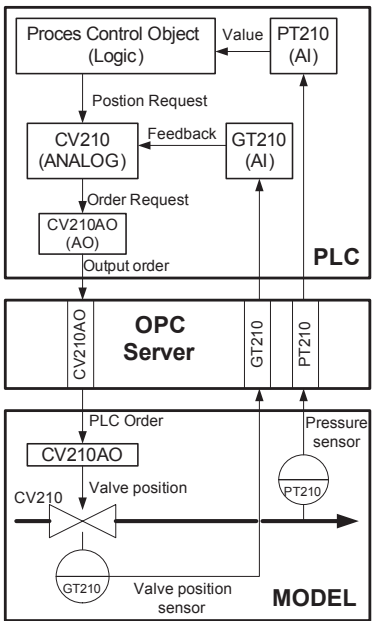

Figure 2: Links between the PLC and the process model

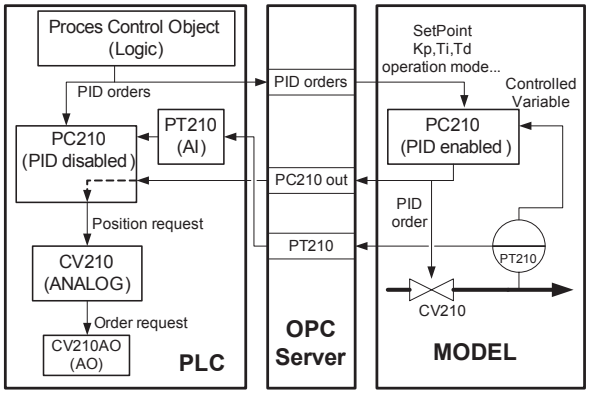

Figure 3: PID controller management in simulator

The simulation speed is not constant, therefore a synchronization between the PLC and the simulation is necessary: PLC ramps and timers are now based on the simulation time. Moreover, PID controllers are not executed in the PLC anymore but directly in the model and main parameters are sent back to the PLC to ensure the consistency in the PLC program and in the supervision, see Fig. 3.

This simulation environment is especially adapted for operator training since the supervision interface remains the same as for the real plant. All LHC cryoplants represent more than 42000 inputs/outputs and around 5000 PID control loops. The use of the same PLC control programs save a lot of development time. Moreover, PLC control programs can be directly validated in their real environment with the possibility to test all interlocks, sequences and closed-loops of the systems.

3. Cryogenic modelling

EcosimPro© allows to model cryogenic systems by using an *object-oriented approach* where each cryogenic component is described by a set of differential and algebraic equations (DAEs). Helium and material properties are obtained by linear interpolations from large properties tables. Material properties are calculated as function of temperatures using some empirical formulations given by Marquardt, Le, and Radebaugh (2000). Helium properties are obtained with the specialized helium library HEPAK© off-line and then integrated in the simulator to increase the simulation speed : interpolations performed in tables are 5 times faster than using

directly HEPAK© online. Properties tables are available for a temperature range between 1 K and 400 K and for a pressure range between 1 kPa and 2.5 MPa including the two-phase region.

3.1. Model Building

A cryogenic library was developed to build easily complex cryogenic systems by drag and drop in the Ecosimpro© graphical user interface. Component models are divided in two main categories:

(a) Pressure components imposing a pressure;

(b) Flow components imposing a mass flow.

First, the cryogenic system must be built in a such way that pressure components are connected to flow components and vice-versa to ensure the overall consistency of the system, i.e. to have as many equations as unknown variables. Figure 4 illustrates the interconnection between a flow component and two pressure components. Then, each component must be parameterized with its own characteristics (e.g., material, design temperature, mass, etc.). Finally, some boundary conditions have to be chosen if the system is not in closed-loop.

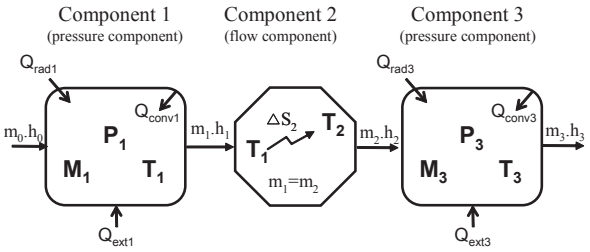

Figure 4: Connections between flow and pressure components

Figure 5 represents a model overview of a small cryogenic system under EcosimPro using a compressor, two heat exchangers, one turbine, five valves, six pipes and one phase separator at the end. Pressure components are colored in yellow and flow components in blue whereas all orange objects are inputs/outputs with controllers that are included in the model and linked to the PLC.

3.2. Pressure components

Pressure components perform isochore transformations and they have uniform pressure and temperature. They represent cryogenic equipments of non-negligible volume like pipes or phase separators.

Table 1: Main thermodynamic and geometric variables

Symbol	Description	Unit
C_p	Specific heat	$J.kg^{-1}.K^{-1}$
E	Energy	J
h	Specific enthalpy	$J.kg^{-1}$
k	Conductivity	$W.m^{-1}.K^{-1}$
Lv	Latent heat of vaporization	$J.kg^{-1}$
Pr	Prandlt number	–
P	Pressure	Pa
s	Specific entropy	$J.kg^{-1}.K^{-1}$
T	Temperature	K
u	Internal energy	$J.kg^{-1}$
x	Mass vapor fraction	%
γ	Specific heat ratio ($\frac{Cp}{Cv}$)	–
μ	Viscosity	$Pa.s$
ρ	Density	$kg.m^{-3}$
$\dot{F}$	Volumetric flow	$m^3.s^{-1}$
hc	Heat transfer coefficient	$W.m^{-2}.K^{-1}$
$\dot{m}$	Mass flow	$kg.s^{-1}$
$\dot{Q}$	Heat flow	W
Re	Reynolds number	–
η	Efficiency	–
D	Diameter	m
L	Length	m
M	Mass	kg
S	Surface; Cross section	m^2
V	Volume	m^3

Pipes

The pipes are characterized by their material, geometry (length and diameter), heat transfer coefficient and eventually their pressure drop coefficient. The following mass and energy balances are performed to compute the internal pressure and temperature:

$$\frac{dM}{dt} = \dot{m}_{in} - \dot{m}_{out} \tag{1}$$

$$\frac{d}{dt}(M \cdot u) = \dot{m}_{in} \cdot h_{in} - \dot{m}_{out} \cdot h_{out} + \sum_i \dot{Q}_i \tag{2}$$

where $\dot{Q}_i$ are the different heat flows applied to the fluid by convection or radiation (conduction is neglected). Convection and radiation heat flows are computed according to:

$$\begin{cases} \dot{Q}_{conv} = h_c \cdot S_W \cdot (T - T_W) = M_W \cdot Cp_W \cdot \frac{dT_W}{dt} \\ \dot{Q}_{rad} = C \cdot (T_{ext}^4 - T^4) \end{cases} \tag{3}$$

where $\dot{Q}_{conv}$ is the convection heat between the fluid and its enclosure and $\dot{Q}_{rad}$ is radiative heat loss. Subscripts $_W$ refers to the metal enclosure (wall), C is a coefficient

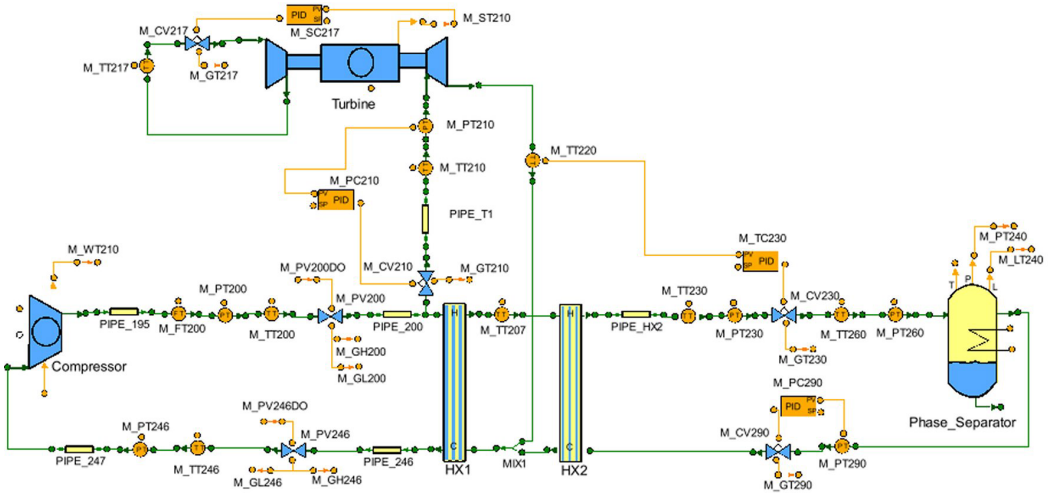

Figure 5: Small cryogenic model overview in EcosimPro

related to the total emissivity of the component and T_{ext} the exterior temperature. The metal heat capacity Cp_w is function of temperature and the heat transfer coefficient hc can be set as a constant or dynamically computed. If necessary, other heat transfers coming from other components or from environment can be added.

If the pipes are long enough or have pressure drop singularities, the pressure drop can be not negligible and in this case this pressure drop is computed by:

$$\Delta P = K \cdot \frac{\dot{m}^2}{2\rho}, \tag{4}$$

where K is the singular pressure drop coefficient depending of the roughness and the geometry of the pipe (length, diameter, elbows...).

Phase separator

The phase separator is filled with a liquid/gas mixture and the liquid falls down due to the gravity. The mixture is considered at the equilibrium point with homogeneous pressure and temperature. There are a diphasic input and a gaseous output at the top, and a liquid output at the bottom. The phase separator is also equipped with an electrical heater at the bottom and all the heat sources (convection, radiation, heater) are applied in the liquid phase only. Hence, the evaporated mass per second can be computed as:

$$\dot{m}_{evap} = \frac{\dot{Q}_{conv} + \dot{Q}_{rad} + \dot{Q}_{eh}}{Lv} \tag{5}$$

where $\dot{Q}_{eh}$ is the power delivered by the electrical heater. The gas and liquid mass balances are defined as:

$$\frac{dM_g}{dt} = \dot{m}_{in} \cdot x_{in} - \dot{m}_{out,g} + \dot{m}_{evap}, \tag{6}$$

$$\frac{dM_l}{dt} = \dot{m}_{in} \cdot (1 - x_{in}) - \dot{m}_{out,l} - \dot{m}_{evap}, \tag{7}$$

where subscripts g and l are referring to the saturated gas and saturated liquid. The gas and liquid energy balances become:

$$\frac{d}{dt}\left(M_g \cdot u_g\right) = \dot{m}_{in} \cdot h_g \cdot x_{in} - \dot{m}_{out,g} \cdot h_{out,g} + m_{evap} \cdot h_g, \tag{8}$$

$$\frac{d}{dt}\left(M_l \cdot u_l\right) = \dot{m}_{in} \cdot h_l \cdot (1 - x_{in}) - \dot{m}_{out,l} \cdot h_{out,l} - m_{evap} \cdot h_l \tag{9}$$

Mass and volume repartitions between gas and liquid are deduced by:

$$\begin{cases} V_l = \frac{M_l}{\rho_l} \\ V_g = V - V_l, \end{cases} \tag{10}$$

and the liquid level z is then computed as:

$$z = \frac{V_l}{V} \cdot L, \tag{11}$$

where L is the height of the tank. Then, the average quality $\bar{x}$, density $\bar{\rho}$ and internal energy $\bar{u}$ are computed to deduce all other thermodynamic properties in the phase separator (pressure, temperature...):

$$\begin{cases} \bar{x} = \frac{M_g}{M} \\ \bar{\rho} = \frac{M}{V} \\ \bar{u} = \bar{x} \cdot u_g + (1 - \bar{x}) \cdot u_l \end{cases} \tag{12}$$

3.3. Flow components

The flow components impose a mass flow according to a pressure drop at their boundaries. Only algebraic equations are used to compute mass flows because flow dynamics are negligible in comparison to thermal dynamics. Thus, there is not any mass accumulation in components and the mass balance is hence defined by:

$$\frac{dM}{dt} = 0 \Leftrightarrow \dot{m}_{in} = \dot{m}_{out}. \quad (13)$$

Valves

Thermodynamic transformation through valves is considered isenthalpic ($h_{in} = h_{out}$) and the mass flow is computed according to a classical CV (valve coefficient) formulation. The input parameters of valve models are their maximum CV, their opening and closing speed and their rangeability (characterize the non-linearity of the opening). Cryogenic valves have generally an equal percentage opening, thus the CV coefficient is computed by:

$$C_V = \frac{CV_{max}}{R} \cdot e^{\frac{u}{100} \cdot log(R)} - \frac{CV_{max}}{R} \cdot (100 - u), \quad (14)$$

where CV_{max} is the CV of the valve for a complete opening, R is the rangeability of the valve (generally $R = 50$) and u is the position of the valve between 0% and 100%. Then, mass flow is given by:

$$\dot{m} = 2.4 \cdot 10^{-5} \cdot C_V \cdot Y \cdot \sqrt{\rho \Delta P}, \quad (15)$$

where Y is either a function of the pressures, either a constant according to the flow regime: $Y = 1 - \frac{\Delta P / P_{in}}{(3 \cdot \frac{\gamma}{1.4} \cdot 0.65)}$ if $\Delta P / P_{in} < \frac{0.65\gamma}{1.4}$ (subsonic flow), else $Y = 2/3$ (sonic flow).

Turbines

Cryogenic turbines are gas turbo-expanders allowing to extract heat into work. They are defined by their design operating point (pressure, temperature, rotational speed, mass flow and efficiency), by their blade diameter D and the inertia momentum of the shaft.

If helium is considered as a polytropic gas, the flow becomes sonic if the pressure ratio $pr = \frac{P_{out}}{P_{in}}$ is above a critical pressure ratio defined by:

$$pr_{crit} = \left(\frac{2}{\gamma + 1}\right)^{\gamma/(\gamma-1)}. \quad (16)$$

An isentropic flow for ideal gas through a nozzle is considered to calculate the turbine mass flow. It is computed from:

$$\dot{m} = m_d \cdot \frac{G}{G_d}, \quad (17)$$

$$G_{sonic} = \sqrt{P_{in} \cdot \rho_{in} \cdot \gamma \cdot \left(\frac{2}{\gamma + 1}\right)^{(\gamma+1.)/(\gamma-1)}}, \quad (18)$$

$$G_{sub} = \sqrt{\frac{2 \cdot \rho_{in} \cdot P_{in} \cdot \gamma}{\gamma - 1} \cdot pr^{2/\gamma} - pr^{(\gamma+1)/\gamma}}, \quad (19)$$

where G is calculated according to the flow regime: (18) is used for a sonic flow and (19) for a subsonic flow. These calculus are ratios between design values represented by subscripts "$_d$" and current values to be sure to obtain good results at the design operating point and remove all constants of the system generally not well known and inducing errors.

If an isentropic expansion is considered ($s_{in} = s_{out}$), the corresponding output enthalpy $hout_s$ can be directly deduced from the output pressure and the entropy. The real output enthalpy $hout$ is computed using an isentropic efficiency:

$$\eta = \eta_d \cdot \left(2 \cdot \frac{v}{v_d} - \left(\frac{v}{v_d}\right)^2\right), \quad (20)$$

$$v = \frac{c_b}{c_j} = \frac{\pi \cdot D \cdot N}{\sqrt{2 \cdot (hin - hout_s)}}, \quad (21)$$

where v is the ratio between the blade velocity (c_b) and the jet velocity (c_j) of the turbine, N is the shaft speed of the turbine and D the diameter of the blade. Considering the isentropic efficiency in the energy balance, the real output enthalpy h_{out} can be computed from:

$$E = \dot{m} \cdot (hin - hout) = \eta \cdot \dot{m} \cdot (hin - hout_s). \quad (22)$$

The shaft speed N is computed by the differential equation:

$$I \cdot N \cdot \frac{dN}{dt} = E - E_d \cdot \left(\frac{N}{N_d}\right)^4, \quad (23)$$

where I is the inertia momentum of the shaft.

Warm compressors

Warm compressors compress gaseous helium at ambient temperature, an isothermal compression is considered here ($T_{in} = T_{out}$). They are volumetric machine, thus the mass flow simply depends on the density of input helium and of the volumetric flow $\dot{F}$ of the compressor which is constant:

$$\dot{m} = \dot{F} \cdot \rho_{in}. \quad (24)$$

Cold compressors

They are non volumetric machines and the model is based on their internal pressure field. This pressure field defines the compressor operating points according to three correlated variables: the pressure ratio, the reduced mass flow and the reduced speed. Several operating points of this pressure field are entered as parameters and the mass flow is computed by interpolations between operating points. The pressure fields are adjusted by a parameter identification made on each compressor to fit experimental operating points. Isentropic efficiencies are also defined from this pressure field and the same method of interpolation is used to calculate the output temperatures, see, for instance, Bradu, Niculescu, and Gayet (2008a) for more details on the cold-compressor model.

3.4. Heat exchangers

Cryogenic heat exchangers (HXs) are generally plate-fin counter-current HXs in brazed aluminum. HXs are composed of different streams which are characterized by their design operating point (temperature, pressure, mass flow, pressure drop, global heat transfer coefficient). The material, the volume and the mass of each stream are also taken into account to have good dynamics. To cope with the complexity of the HX and to take into account the dynamics along the streams, a space discretization is performed on each stream which is divided in N nodes, see Fig. 6.

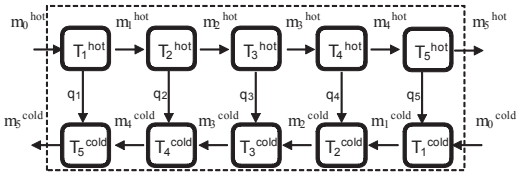

Figure 6: Heat exchanger model

Equations (1), (2) and (3) previously defined for pressure components are used to estimate the temperature of each nodes and a term q_i is added in (2) to compute the convective heat fluxes between hot and cold streams. This term is calculated using a logarithmic mean temperature difference method (LMTD):

$$q_i = hc_i \cdot \frac{\Delta T_{i+1} - \Delta T_i}{log\left(\frac{\Delta T_{i+1}}{\Delta T_i}\right)} \tag{25}$$

with $\Delta T_i = T_i^{hot} - T_{N-i+1}^{cold}$ and the global heat transfer coefficient hc_i in a node is computed on the basis of the empirical formulation of Colburn, especially adapted for turbulent flow in HXs (Colburn, 1933):

$$hc_i = \frac{k_i}{D} \cdot 0.023 \cdot Pr_i^{1/3} \cdot \left(\frac{\dot{m}_i \cdot D}{\mu_i}\right)^{0.8}. \tag{26}$$

Many phenomena occur in HXs and the empirical formulations used do not take into account complex geometries. For those, other methods exist to compute global heat transfer coefficients according to the HX type. These methods imply a perfect knowledge of the equipments and the formulas are specific to each configuration. To cancel the geometrical constant D generally not known and to avoid static error at the design operating point, the ratio between the (26) and the design global heat transfer coefficient hc_d, known and guaranteed by suppliers is performed:

$$hc_i = \frac{hc_d}{N} \cdot \frac{k_i}{k_d} \cdot \left(\frac{\dot{m}_i \cdot \mu_d}{\dot{m}_d \cdot \mu_i}\right)^{0.8} \cdot \left(\frac{\mathrm{Pr}_i}{\mathrm{Pr}_d}\right)^{1/3} \tag{27}$$

to compute the global heat transfer coefficient as function of design values identified by the subscripts 'd'.

In other simulation approaches, Kutzschbach et al. (2006); Deschildre et al. (2008) use an equation based on the Colburn formulation by adjusting parameters related the type of HXs. Next, Maekawa et al. (2005) makes also a ratio with the design heat transfer coefficient and it considers a constant conductivity, viscosity and Prandl number.

The mass flows between each node are deduced from the friction equation given by:

$$\Delta P = fr \cdot \frac{\dot{m}^2 \cdot L}{S^2 \cdot 2 \cdot D \cdot \rho}, \tag{28}$$

where $fr = 0.184 \cdot Re^{-0.2}$ is the Darcy friction factor.

The same method is used to remove all geometrical parameters and empirical constants. Finally the following equation using the known design values is obtained:

$$\Delta P = \Delta P_d \cdot \left(\frac{\dot{m}}{\dot{m}_d}\right)^{1.8} \cdot \left(\frac{\mu_d}{\mu}\right)^{-0.2} \left(\frac{\rho_d}{\rho}\right). \tag{29}$$

3.5. Numerical solvers

The numerical solvers embedded in the software EcosimPro are used to solve the differential and algebraic equations (DAEs) of the form:

$$F(t, y(t), \dot{y}(t)) = 0 \tag{30}$$

The following steps are performed to solve the entire system at each integration step:

- Symbolic solutions of independent linear equations are found;
- Subsets of linear systems are detected and solved by a linear equations system solver;
- Subsets of non-linear systems are detected and solved by a tearing technique which performs iterations on some selected tearing variables to calculate unknowns as function of theses variables;
- Then, the DAE system is solved by a DASSL algorithm (Petzold, 1984).

4. Simulation results

The different cryogenic components described previously were used to model different CERN cryogenic systems. All simulations are performed in closed-loop as on real plants, the PLC give the different orders to actuators and controllers, there is no experimental data included in simulations. Nevertheless, some manual operations can be reproduced in simulations (set-point changed manually, valve forced by operators, etc.).

4.1. CMS cryoplant

The first cryogenic system modeled and simulated is the cryoplant of the particle detector CMS where a large superconducting magnet of 225 tons has to be cooled at 4.5 K with liquid helium. The CMS cryoplant is composed of a compression station, a helium cold-box (refrigerator) and a coil cryogenic system as it is shown in Fig. 7.

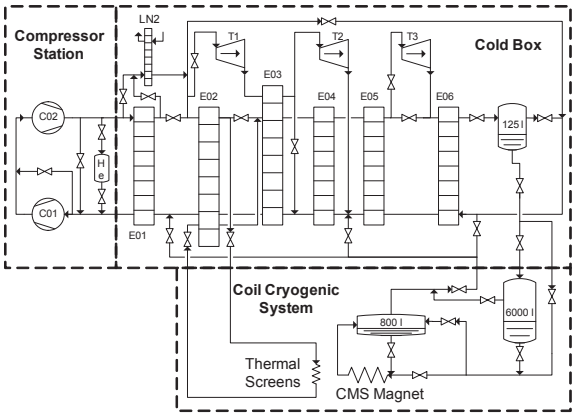

Figure 7: The CMS cryoplant

The model of the entire plant under EcosimPro© is made of 3080 DAEs containing 219 derivatives. Around 30 control loops and more than 300 inputs/outputs are simulated in the PLC.

First simulations have been performed with the cold-box alone. The dynamic behavior simulated agrees to the one observed on the real plant as it is shown on the first graph of the Fig. 8 where the simulated temperature at the beginning and at the cold-end of the cold-box is plotted and compared with a real cool-down achieved in January 2008. The maximum relative error observed in simulation on temperatures, pressures and mass flows is about 5% around turbines.

The second graph of the Fig. 8 shows the temperature after the first HX during a manual action on the turbine inlet valve performed in February 2006 (the first cool-down of the magnet) and reproduced in simulation. The good agreement between the real and the simulated behavior shows that the global dynamic response of the plant is correct. Note that the delay between the pre-cooler stop on the real plant and in the simulation comes from the difference of the cool-down speed due to the under-estimation of the cold-mass.

4.2. 1.8 K refrigeration unit for the LHC

A 1.8 K refrigeration unit for the LHC was also simulated. This unit is used to cool-down the LHC magnet helium baths from 4.5 K down to 1.8 K following the saturation line of helium. These units pump gaseous helium over 3.3 km sector from atmospheric pressure until 1.6 kPa using cold-compressors, see Fig. 9. The entire model contains 3056 DAEs with 249 derivatives and 150 inputs/outputs are simulated with 14 control loops.

Similarly to the previous case study, the simulation agrees with the real data acquired during the final cool-down of the sector 5-6 of the LHC achieved in April 2008, see Fig. 10. Transients are well simulated and the control of cold compressors is well reproduced. The output temperatures of cold compressors are lower in simulation than on the real plant due to isentropic efficiencies which are over-estimated in the model.

The simulator was also used to test a new set-point management for cold compressors avoiding steps on compressor speeds. As simulation shows a real improvement, with a smoother control and lower constraints on machines, see Fig. 11, this new set-point management was successfully implemented on the real plant.

4.3. Warm compressor stations for the LHC

Warm compressor stations are composed of several volumetric compressors working at ambient temperature. They compress gaseous helium from atmospheric

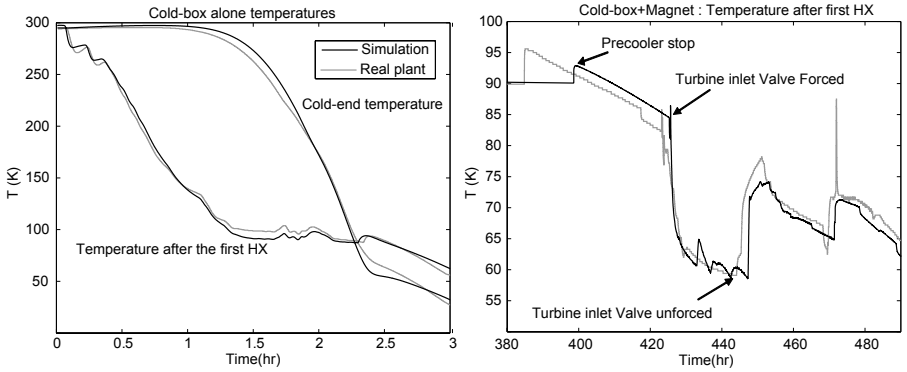

Figure 8: Comparison between experimental and simulated temperatures during a cool-down of the cold box alone and with the CMS magnet

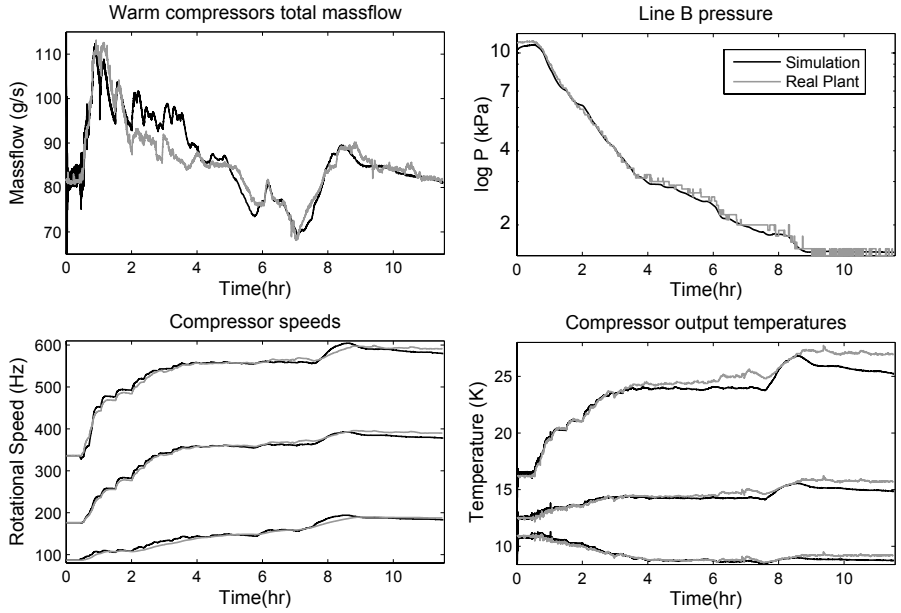

Figure 10: Comparison between experimental and simulated main variables during the pumping from 10 kPa to 1.6 kPa of a LHC sector

pressure up to 1.8 MPa. A model of a LHC warm compressor station was elaborated to test an Internal Model Control for the high pressure regulation on which classical PI controllers are not adapted (Bradu, Niculescu, and Gayet, 2009).

An Internal Model Control (IMC) with 2 degrees of freedom was developed: one degree to follow the set-point and one degree to compensate unmeasured disturbances. An anti-windup system to take into account saturations of actuators (valves) was also included, see Zheng, Kothare, and Morari (1994) for details. Moreover, a feed-forward action was added to take into account a measurable disturbance. Note that the internal model of the controller was obtained by a parameter identification made on the simulator because it was not possible to perform an identification procedure on the real plant for availability and safety reasons.

Two simulations were performed to compare the former PI controller and the IMC controller during a turbine stop that constitute an important disturbance on the high pressure, see Figure 12. Oscillations in steady-state were removed and the disturbance rejection is efficient as the overshoot, initially of 8%, was reduced to less than 2% and the recovery time passed from 40 minutes with the PI controller to 10 minutes with the IMC controller. The IMC has not been tested yet on the real plant because the system is currently in operation but some experimental tests should be done in future.

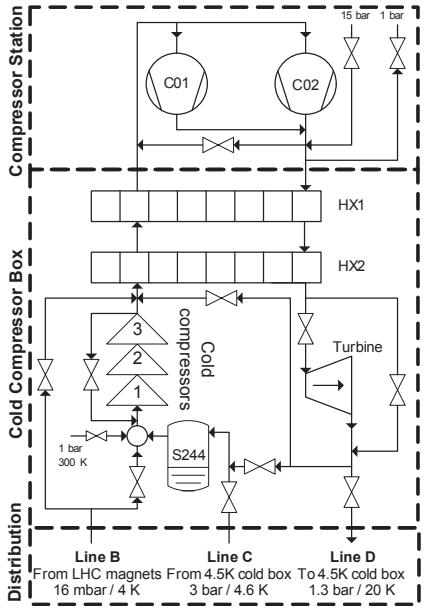

Figure 9: A 1.8 K refrigeration unit for the LHC (Air Liquide)

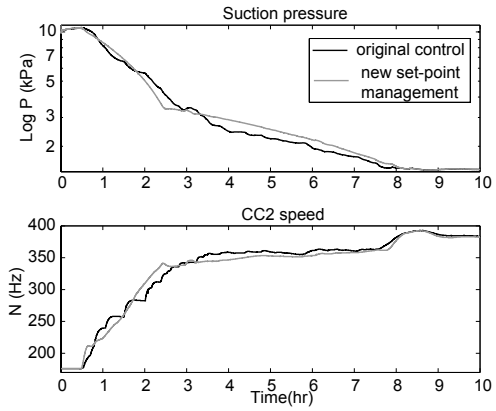

Figure 11: Comparison between the former and the new pressure set-point management of cold compressors

4.4. Simulation speed

Simulations are performed on a classical computer, a Pentium© D 3.4 GHz with 1GB of RAM. The simulation speed is highly dependent on the communication interval of the integration (the frequency with which data are available for the PLC and for the plots), on the number of DAEs, derivative variables and coupled linear subsystems which are generating a lot of computation. A HX stream divided in N nodes generates $N+1$ derivative variables and one coupled linear subsystem of N equations. Hence, the simulation speed is directly linked to the total number of HX nodes.

After various simulations and comparisons, it was observed that a communication interval of 2 seconds is sufficient to simulate the fastest dynamics between the model and the PLC and to have a sufficient number of points in plots. Moreover, it was noticed that for classical plate-fin HXs (between 300 K and 6 K), streams have to be divided in 5 nodes minimum to appreciate the spatial dynamic. On the basis of the above considerations, the trade-off between the computational time and the precision is in agreement with the requirements : simulations are much faster than real-time. The Table 2 compares simulation speeds during the cool-down and a 1.8 K refrigeration unit for the LHC (QURC). Each system is simulated in different configurations : alone, with its warm compression station (WCS) or with its thermal load. Note that for operator training, it is possible to activate a real-time option.

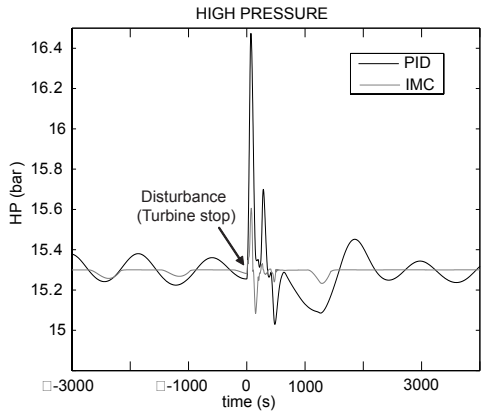

Figure 12: Comparison in simulation between PID and IMC control

Table 2: Simulation speed average during cool-down phase

System	DAE[a]	Der[b]	Sys[c]	Spd[d]
TCF50	1786	146	10	x18
TCF50+WCS	2050	175	11	x15
CCB	2581	205	14	x14
CCB+WCS+load	3334	296	16	x8
QURC+WCS	1921	147	6	x130
QURC+WCS+load	3056	249	6	x83

[a] Number of differential-algebraic equations
[b] Number of derivative variables
[c] Number of coupled linear sub-systems
[d] Simulation speed (ratio to real time)

5. Concluding remarks and perspectives

The tools and methods used for these simulations are close to those used in continuous processes like in

petroleum or sugar industries (see for instance Alves et al. (2005)), and the different constraints related to cryogenic specificities was introduced. Cryogenic components have been designed and tested successfully with different CERN cryogenic systems. The simulation environment PROCOS proved its ability to conduct pertinent dynamic simulations for large-scale cryogenic systems during a complete cool-down phase.

Errors mainly come from bad component parameters (e.g., thermal efficiency, volume, etc.), model approximations (e.g., conduction neglected) and unknown pressure drops due to complex geometries (e.g., pipe network). Some component parameters not well known such as design pressure drops have been adapted to cope with real data. Moreover, some empirical characteristics as pressure fields of compressors can be corrected using parameter identification experimentally. Uncertainties on helium and material properties are minimal and do not imply significative errors, excepting in the helium supercritical region. It was also noticed that the modelling of large volumes and metal mass is very important to obtain good dynamics illustrated by some delay and buffer effects even if volumes and masses are generally not well known in such large-scale cryogenic systems.

The simulator was also used for different purposes and showed its flexibility. For instance, it was used to perform a virtual PLC commissioning on the CERN central helium liquefier, allowing developers to debug the control program before its implementation on the real plant. This method proved its interest by the gain obtained in terms of running time.

Then, a new set-point management for cold-compressors was tested in simulation and successfully implemented on the LHC cryogenic system. In addition, the simulator was used as a test bench to test a new Internal Model Control on a warm compressor station and the internal model of the controller was identified parametrically using the simulator.

Finally, a special room will be available soon at CERN to train people on the cryogenic operation on the CMS cryoplant and on the 1.8 K refrigeration unit for the LHC.

In the future, the remaining components of the LHC cryogenic systems will be modeled, especially the 18 kW @ 4.5 K refrigerators and the thermal load related to the LHC magnets.

Acknowledgments

The authors would like thank the CERN cryogenic group in Geneva who supported this work as well as the anonymous reviewers of Control Engineering Practice whose comments and pertinent remarks helped us to improve the overall contribution of the paper.

References

Alves, R., Normey-Rico, J., Merino, A., Acebes, L., de Prada, C., 2005. Opc based distributed real time simulation of complex continuous processes. Simulation Modelling Practice and Theory 13(7), 525–549.

Blanco, E., de Prada, C., Cristea, S., Casas, J., 2009. Nonlinear predictive control in the LHC accelerator. Control Engineering Practice, In Press.

Bradu, B., Niculescu, S.-I., Gayet, P., 2008a. Dynamic simulation of a 1.8 K refrigeration unit for the LHC. In: Proceedings of the 22nd ICEC. pp. 525–530.

Bradu, B., Niculescu, S.-I., Gayet, P., 2008b. Modeling, simulation and control of large scale cryogenic systems. In: Proceedings of the 17th IFAC World Congress. pp. 13265–13270.

Bradu, B., Niculescu, S.-I., Gayet, P., 2009. Control optimization of a LHC 18 kW cryoplant using dynamic simulations. Advances in Cryogenic Engineering, In Press.

Butkevich, I., Idnic, E., Shpakov, V., 2006. Cryogenic helium units simulation model. In: 21st International Cryogenic Engineering Conference. Prague, Czech Republic, pp. 223–226.

Colburn, A., 1933. A method of correlating forced convection heat transfer data and a comparison with fluid friction. Transactions of the American Institute of Chemical Engineers 19, 174–210.

Deschildre, C., Barraud, A., Bonnay, P., Briend, P., Girard, A., Poncet, J., Roussel, P., Sequeira, S., 2008. Dynamic simulation of an helium refrigerator. Advances in Cryogenic Engineering 53, 475–482.

EA Internacional, 2007. EcosimPro 4.4: Mathematical algorithms and simulation guide. Madrid, Spain.

Gayet, P., Barillère, R., 2005. UNICOS : a framework to built industry-like control systems, principles and methodology. In: International Conference on Accelerator and Large Experiment Physics Control Systems. Geneva, Switzerland.

IEC, 1997. Standard IEC 61512-1, Batch control. Part 1: Models and terminology.

Kutzschbach, A., Haberstroh, C., Quack, H., 2006. Dynamic simulation of a helium liquefier. In: 21st International Cryogenic Engineering Conference. Prague, Czech Republic, pp. 219–222.

Lebrun, P., 1999. Cryogenics for the large hadron collider. IEEE Transactions on Applied Superconductivity 10, 1500–1506.

Maekawa, R., Ooba, K., Nobutoki, M., Mito, T., 2005. Dynamic simulation of the helium refrigerator/liquefier for LHD. Cryogenics 45, 199–211.

Marquardt, E., Le, J., Radebaugh, R., 2000. Cryogenic material properties database. In: Proceedings of the 11th International Cryocooler Conference. pp. 681–687.

Olsen, I., Endrestol, G., Sira, T., 1997. A rigorous and efficient distillation column model for engineering and training simulators. Computer chemical Engineering 21, 193–198.

Petzold, L., 1984. A description of DASSL: a differential-algebraic system solver. Sandia National Laboratories.

Szafnicki, K., Narce, C., Bourgois, J., 2004. Towards an integrated tool for control, supervision and operator trainingapplication to industrial wastewater detoxication plants. Control Engineering Practice 13, 729–738.

Zheng, A., Kothare, M., Morari, M., 1994. Anti-windup design for internal model control. International Journal of Control 60, 1015–1024.